

Optimum Shape Design of Metal-Enclosed 550 kV Disconnectors Based on Response Surface Method and Finite Element Analysis

Ruilei Gong

School of Electrical
Engineering, Xi'an
Jiaotong University,
Shaanxi, Xi'an, 710049,
China

Shuhong Wang

School of Electrical
Engineering, Xi'an
Jiaotong University,
Shaanxi, Xi'an, 710049,
China

Xianjue Luo

School of Electrical
Engineering, Xi'an
Jiaotong University,
Shaanxi, Xi'an, 710049,
China

Michael G. Danikas

Department of Electrical
and Computer
Engineering, Democritus
University of Thrace,
67100 Xanthi, Greece

Abstract— In this paper, the optimum shape design of 550 kV disconnectors in Gas Insulated Switchgears (GIS) are firstly presented employing the Finite Element Method (FEM) for electric field analysis coupled with an optimal design method. For effective analysis, the FEM is conducted in transient quasistatic electric field, using a finite element FORTRAN code. The structure parameters of disconnectors that provide the required electric field strength are obtained by the Response Surface Method (RSM) and the optimal values are presented by the variation in maximal electric field strength. The RSM and optimal design methods are also conducted by FORTRAN codes. The optimal result reveals that a uniform electric field distribution is achieved in 550 kV disconnectors. Additionally, the optimal result of disconnectors is verified by the proposed disconnector undertaken power frequency withstanding voltage of 740 kV for 1 minute, lightning impulse of 1675 kV, and operating impulse of 1300 kV, respectively.

Keywords—Disconnectors; response surface method (RSM); optimization; structure design; finite element method (FEM)

I. INTRODUCTION

Disconnectors in Gas Insulated Switchgears (GIS) are a switching device without an arc extinguishing device. An opened state should be obvious (visible) and a breakdown is not allowed under any circumstances, in order to ensure the safety of the maintenance personnel. Furthermore, disconnectors in the closed state must reliably carry normal and/or short circuit currents. Because of the special role of disconnectors, there is the need to consider its two working states: the opened state, to meet the insulation design, and the closing state, to meet the through flow capacity design and insulation design. Therefore, the insulation of disconnectors design is essential.

The insulation performance of disconnectors mainly depends on the electric field distribution in the breaking. The electric field distribution in the breaking state is directly related with the structure shape of shielding. Therefore, the optimization of disconnectors mainly concerns the optimization of the shielding structure. Because of the structural complexity

of disconnectors, it is difficult to determine the field distribution in the inside, and therefore a Finite Element Method (FEM) is employed [1-2]. 3D modeling is more realistic but due to the axial symmetry, a simplified two-dimensional calculation can be considered not to affect the analysis results. Herein, a commercial software is used and it is compared with a simplified two-dimensional calculation and three dimensional calculation and analysis. The result reveals that the simplified model meets the accuracy required. In addition, the model of disconnectors employs a two-dimensional model of transient quasistatic electric field considering the conductivity and permittivity of materials in order to obtain more accurate results.

At present, several optimization methods, e.g. genetic algorithms and the simulated annealing method, have been used in combination with FEM, but they usually suffer from low efficiency. The Response Surface Method (RSM) has been successfully combined with FEM as an efficient way to realize the optimization of structure parameters of different electric devices [3-5]. RSM uses discrete points obtained according to some experimental design rules and constructs the optimal approximate function to attain optimal results. RSM combined with FEM can effectively reduce the calculation and workload, and also obtain high accuracy results. In this paper, this is the first time that RSM and FEM are successfully applied to the optimization of a high-voltage disconnector in GIS. Additionally, in order to realize optimization analysis for automatic calculation, RSM, FEM and subsequent optimization algorithm programs are written using the FORTRAN language.

II. TRANSIENT QUASISTATIC ELECTRIC MODEL

Analysis of the internal electric field of disconnectors, due to the lightning impulse voltage, is a function of time as well as of the conductivity of the insulating medium. Therefore, this paper adopts the quasi-static electric field model for transient analysis. A transient electric analysis determines the effects of time-dependent current or voltage excitation in electric devices. For this reason, the time-varying electric and magnetic fields

are uncoupled, and the electromagnetic field can be treated as quasistatic [2, 6-8].

In a quasistatic electric model, the circulation of the electric field is essentially zero for any path; this allows the electric field \vec{E} to be represented by a scalar potential function φ as:

$$\vec{E} = -\nabla\varphi \quad (1)$$

The potential function φ is continuous in the domain, i.e. there are no charge double layers. From the Ampere-Maxwell equation follows that:

$$\nabla \cdot \vec{J} + \frac{\partial(\nabla \cdot \vec{D})}{\partial t} = 0 \quad (2)$$

where \vec{J} is the conduction current density and \vec{D} is the electric displacement.

We assume that at $t=0$ there are no 'free charges' in the system. The electric displacement in the linear isotropic materials is simply related to the electric field:

$$\vec{D} = \varepsilon \vec{E} \quad (3)$$

In the nonconducting regions, from (1), (2) and (3) follows that the Laplace equation for the potential holds:

$$\nabla \cdot (-\varepsilon_0 \varepsilon_j \nabla \varphi) = 0 \quad (4)$$

where ε is the permittivity of free space and ε_j is the relative permittivity of the insulating material.

In the materials considering the conductivity, the current density and the electric field are related by:

$$\vec{J} = \gamma(E) \vec{E} \quad (5)$$

where $\gamma(E)$ is a field dependant conductivity. In the regions considering conductivity, from (1), (2), (3) and (5) it follows that the dynamics of the electric potential is described by a diffusion-like equation:

$$\nabla \cdot [-\gamma(E) \nabla \varphi] = \frac{\partial}{\partial t} [\nabla \cdot (\varepsilon_0 \varepsilon_j \nabla \varphi)] \quad (6)$$

In order to analyze the field distribution of the conductive materials, (6) can be discretized by applying the backward Euler method:

$$\nabla \cdot [-\gamma(E(t)) \nabla \varphi(t)] = \varepsilon_0 \varepsilon_j \frac{\nabla^2 \varphi(t) - \nabla^2 \varphi(t - \Delta t)}{\Delta t} \quad (7)$$

where t is the time and Δt is a suitable small time interval. Equation (7) can be rewritten as:

$$\nabla \cdot [-\gamma(E(t)) + \frac{\varepsilon_0 \varepsilon_j}{\Delta t}] \nabla \varphi(t) = -\varepsilon_0 \varepsilon_j \frac{\nabla^2 \varphi(t - \Delta t)}{\Delta t} \quad (8)$$

Summarizing, (4) and (8) can be written as:

$$-\nabla \cdot [c(\varphi) \nabla \varphi] - f = 0 \quad (9)$$

where

$$c(\varphi) = \begin{cases} \varepsilon_0 \varepsilon_j & \text{in insulating materials} \\ \gamma(E(t)) + \varepsilon_0 \varepsilon_j / \Delta t & \text{in conductive materials} \end{cases}$$

$$f = \begin{cases} 0 & \text{in insulating materials} \\ \gamma(E(t)) + \varepsilon_0 \varepsilon_j / \Delta t & \text{in conductive materials} \end{cases}$$

$$f = \begin{cases} 0 & \text{in insulating materials} \\ -\varepsilon_0 \varepsilon_j \nabla^2 \varphi(t - \Delta t) / \Delta t & \text{in conductive materials} \end{cases}$$

The electric field distribution in disconnectors is symmetric. By adopting a cylindrical reference system with the z-axis coincident with the axis of the conductor of disconnector, the variational problem of (9) is shown as:

$$\begin{cases} F(\varphi) = 2\pi \left(\int_S \left(\int_0^E c(\varphi) \vec{E} \cdot d\vec{E} \right) r dr dz - \int_S f \varphi r dr dz \right) \\ \varphi|_l = \varphi_0 \end{cases} \quad (10)$$

The corresponding finite element equation is:

$$K(\varphi)\varphi = P(\varphi) \quad (11)$$

where $K(\varphi)$ is the $n \times n$ nonlinear matrix, φ is the n column vector of the nodal potentials, and $P(\varphi)$ is the sum of the n column vector produced by dealing with Dirichlet boundary conditions and produced by equivalent charge density.

Equation (11) can be iteratively solved by means of the Newton-Raphson method. Starting from a guess ϕ^n of the solution, an improved approximation ϕ^{n+1} is obtained by solving the series linearized problem. This iterative algorithm is repeated until the condition

$$\frac{|\phi^{n+1} - \phi^n|}{|\phi^n|} \leq \chi \quad (12)$$

is verified. χ is a prescribed small value, and the corresponding value ϕ^{n+1} is assumed as the solution of the system at time instant t . The solution at time instant $t + \Delta t$ could be finished through solving (11). And last, in all time domains the solution can be attained.

This numerical model represents an improvement of the quasistatic electric field approach presented in [9] for two main

reasons. The first one concerns that the model can finish the transient electric field analysis. And the second is that the model considers the conductivity of the material, thus providing more accurate results.

III. RESPONSE SURFACE METHOD

The response surface method (RSM) is a powerful tool to build up a macro model for an approximation of the desired system response. The main advantage in this macro model would be the significant reduction of the needed number of simulations to characterize the electric insulation performance of disconnectors, and thus make the electric field optimization of disconnectors feasible and efficient. The macro model generally comprises a simple, mathematical expression that describes the desired objective or response, obtained from either measurements or simulations, as a function of the specified design parameters, which are the input variables to the simulations. The expression is usually one, two or higher degrees of the design parameters. The technique engaged in model fitting is originally stemmed from the design of experiments techniques. The computational cost needed for deriving the expression is orders of magnitude much less than that needed for simulations. Once this expression is obtained, it can be used to replace the simulations, and furthermore, it makes feasible for the search of the optimal combinatorial set of design parameters that minimize the desired goal.

A. Basic Principles

Constructing the response surface model requires an iterative process. In this study, numerical simulation that adopts the FE analysis is applied to carry out the maximum of electric field strength associated with selected design points, which are needed to fit all the coefficients in the regression model. First define $\beta_j (j=0,1,\dots,k)$ the coefficients of the regression model and ε the error. By further assuming that there are N numerical experiments ($N > k$), the variance of the error ε is equal to σ^2 and each ε is a random variable, the relation between the dependent response T and the independent variables $\hat{X} = x(x_1, x_2, \dots, x_k)$ can be denoted as:

$$\hat{X}\beta = T - \varepsilon. \quad (13)$$

By further performing the minimization of the least square error norm of the random error vector, the regression model can be derived as:

$$\tilde{Y} = \hat{X}b \quad (14)$$

where \tilde{Y} is the estimated response and b the estimated solution of the regression coefficients to this minimization problem, denoted as:

$$b = (\hat{X}^T \hat{X})^{-1} \hat{X}^T T \quad (15)$$

where \tilde{Y} is the estimated response and b the estimated solution of the regression coefficients to this minimization problem, denoted as:

$$b = (\hat{X}^T \hat{X})^{-1} \hat{X}^T T \quad (16)$$

Note that the mathematical expression can be linear or nonlinear. The choice of the degree of the assumed polynomial model would be dependent of the number of simulations to be performed and the desired accuracy. In fact, it would not be practical in real applications to have a polynomial degree greater than 2 because of the significant increasing of the number of simulations. For one degree of polynomial expression, it is presented as

$$y = \beta_0 + \sum_{j=1}^k \beta_j x_j + \varepsilon \quad (17)$$

where y is the response, $x_j (j=1,2,\dots,k)$ the independent variables, $\beta_j (j=0,1,\dots,k)$ the coefficients of the regression model, which are to be determined using regression analysis techniques, and ε the random error. As the numerical simulators are deterministic, the error would only emanate from the fitting inaccuracy. Furthermore, when the linear regression model is incapable of accurately describing the response as function of the specified design variables, the nonlinear regression model can be then attempted. A quadratic regression model with k independent variables is denoted as

$$y = \beta_0 + \sum_{j=1}^k \beta_j x_j + \sum_{i=1}^k \sum_{j=1}^k \beta_{ij} x_i x_j + \varepsilon \quad (18)$$

The experimental design plan used in this work is the Central Composite Design (CCD) proposed by Box and Wilson [10]. It is essentially an orthogonal one such that it would allow a better estimation of the coefficients of the regression model. It consists of all the two-level factorial points, the central point and the axial points or star points. In total, there are 2^k factorial points, $2k$ axial points and a central point in a CCD model, where k is the number of independent design variables. Basically, the model is formed by two parts:

- 1) two-level factorial points with an added central point;
- 2) the symmetrical star points aligned in the axes of the factors and the central point.

Note that the first part can provide the estimation of the first order and two-factor interaction polynomial terms while the second part can allow the fit of the quadratic terms. Once the important design parameters are determined, a complete CCD plan for design parameters can be then defined. The experimental design plan used for a 2-independent-variable system is specifically listed in Table I where x_1 and x_2 are the independent variables, $y (i=1,2,\dots,n)$ the desired response,

and “+1” is the upper limit, “-1” the lower limit, and “0” the central point of the independent variables.

B. Statistical Tests

It would be generally required to check the validity of the mathematical expression constructed from the regression analysis, and also the importance of the included factors. One of the possibilities is to examine the relative and absolute errors between the exact analysis and the responses based on the mathematical expression. Other can be sought through statistical tests. In this context, two simple statistical hypothesis-testing procedures, including *F*-test and *R*² test, are used to get a basic indication of the validity of the constructed model. The *F*-test that basically adopts the analysis of variance examines the significance of the regression model while the *R*² test provides an informal indication of how well the estimated regression model describes the relationship between the independent and dependent variables. In other words, the *R*² gives the fraction of variation accounted for by the regression model fit to the observed data. Moreover, the verification of the regression model is also tested by a new selected design point that is not included in the fit.

In *F* statistics, the statistical index *F*₀ is defined as

$$F_0 = \left(\frac{SSR}{k} \right) \left(\frac{SSE}{(N-k-1)} \right) \quad (19)$$

where *N* is the total selected design points in the experimental design plan, *k* denotes the number of independent design variables in the model, *SSR* expresses the sum of squares due to regression, and *SSE* is the sum of squares due to residual. Accordingly, the total sum of squares *SST* can be expressed as:

$$SST = SSR + SSE = T^T T - \frac{\left(\sum_{i=1}^N y_i \right)^2}{N} \quad (20)$$

where *y_i* is the *i*-th actual response. If *F*₀ > *F*_{α,k,N-k-1}, where α is the specified significance level in the *F* distribution, the null hypothesis, *H*₀ is shown in the following two-sided hypotheses:

$$H_0: \beta_1 = \beta_2 = \dots = \beta_k = 0$$

and

$$H_1: \beta_j \neq 0 \text{ for some } j \text{ in } \{j=1,2,\dots,k\} \quad (21)$$

is rejected, implying that at least one independent design variable is significant to estimated response.

In the *R*² test, the coefficient of multiple determinations *R*² is defined as:

$$R^2 = \frac{SSR}{SST} = 1 - \frac{SSE}{SST} \quad (22)$$

Note that 0 ≤ *R*² ≤ 1. If β_{*j*}(1,2,...,k) = 0, then *R*² = 0.

Furthermore, if all responses derived from the exact numerical simulations are fully equivalent to the estimated responses, then *R*² = 1, suggesting that the fit of the least square line to the data points is perfect.

TABLE I. EXPERIMENTAL DESIGN PLAN OF TWO-INDEPENDENT-VARIABLE SYSTEM

| | <i>x</i> ₁ | <i>x</i> ₂ | Result |
|---|-----------------------|-----------------------|-----------------------|
| 1 | +1 | +1 | <i>y</i> ₁ |
| 2 | +1 | -1 | <i>y</i> ₂ |
| 3 | -1 | +1 | <i>y</i> ₃ |
| 4 | -1 | -1 | <i>y</i> ₄ |
| 5 | +1.414 | 0 | <i>y</i> ₅ |
| 6 | -1.414 | 0 | <i>y</i> ₆ |
| 7 | 0 | +1.414 | <i>y</i> ₇ |
| 8 | 0 | -1.414 | <i>y</i> ₈ |
| 9 | 0 | 0 | <i>y</i> ₉ |

IV. THE MODEL OF DISCONNECTORS

The structural model of disconnectors in GIS is shown in Figure 1, where the horizontal break is of disconnectors, and the vertical break is of the earthing switch. The analysis model in disconnectors can be simplified to a two-dimensional one without affecting the calculation results. The disconnector model for the simplified two-dimensional analysis is shown in Figure 2, and the key parts of disconnectors are marked. The relative permittivity and conductivity of each part are given in Table II, in order to finish finite element calculation under the lightning impulse voltage. Lightning impulse voltage waveform applied on the conductor is shown using the following function [11].

$$e(t) = 1675 \cdot (e^{-\frac{t}{T_1}} - e^{-\frac{t}{T_2}}) \quad (23)$$

where *T*₁ = 68μs, *T*₂ = 0.4μs.

V. THE ELECTRIC FIELD ANALYSIS IN DISCONNECTORS

In Figure 2, several parameters, which may have an effect on the electric field distribution, have been described. The original parameters of disconnectors are listed in Table III.

According to relative standards, lightning impulse withstand voltage with 1675 kV peak value should be applied on one side of the break in the disconnectors, the opposite peak value of power frequency withstand voltage 450 kV applied on the other side. The disconnector model with original parameters was solved using a FORTRAN. The potential distributions and electric field distributions are depicted in Figure 3.

TABLE II. THE RELATIVE PERMITTIVITY AND CONDUCTIVITY OF EACH PART

| | Conductor and shield | Metal part | insulation | SF ₆ |
|----------------|----------------------|-------------------|---------------------|-----------------|
| ϵ_j | - | - | 3.3 | 1 |
| γ (s/m) | 3.5×10^7 | 3.5×10^7 | 1×10^{-13} | 0 |

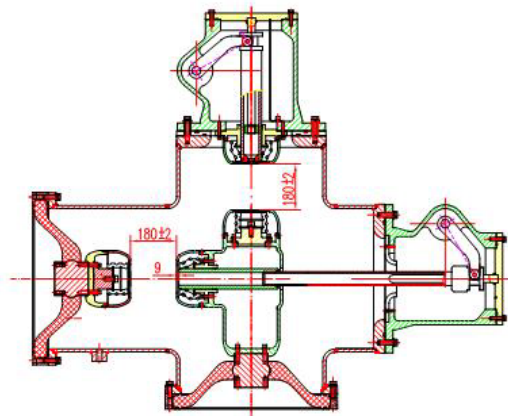


Fig. 1. Structural model of disconnectors

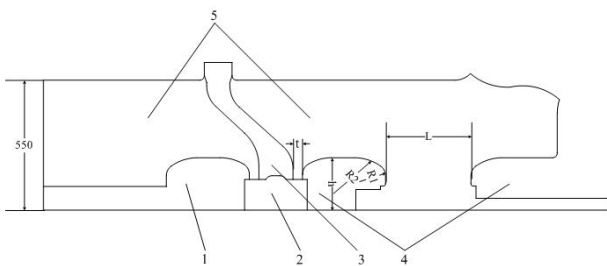


Fig. 2. Simplified model of disconnectors (1,4-the conductor and the shield, 2-the metal part, 3-the insulation, 5-SF₆)

TABLE III. THE DESIGN PARAMETERS OF DISCONNECTORS (MM)

| parameters | L | h | t | R_1 | R_2 |
|---------------|-----|-----|-----|-------|-------|
| Initial value | 180 | 111 | 20 | 25 | 95 |

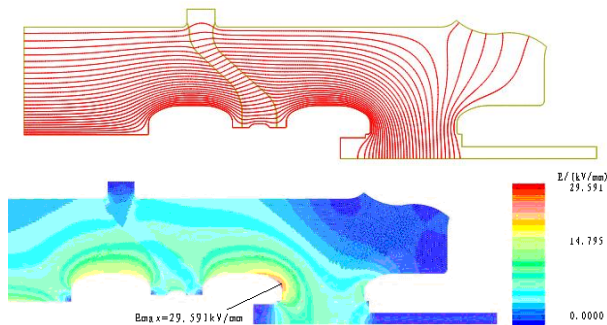


Fig. 3. The potential distribution and field distribution in the model of disconnectors

As shown in Figure 3, the maximal electric field strength is 29.591 kV/mm with the reference value being 24 kV/mm in [12] (when the gauge pressure value of SF₆ is 0.4 MPa, the reference value can be computed). The results indicate that the design of disconnectors should be modified because the maximum electric field strength value has exceeded the allowable value.

In Figure 2 and Table III the several main design parameters are shown. Next, the present study focuses on the change of electric field by altering the design parameters. The relative results are listed in Table IV to VI.

a) Altering parameter t , which is the distance between the contact and insulation (Table IV). The results show that parameter t has almost no effect on the maximal electric field strength in disconnectors.

TABLE IV. THE RELATION BETWEEN PARAMETER t AND THE MAX ELECTRIC FIELD STRENGTH

| Parameter t (mm) | E_{max} (kV/mm) |
|--------------------|-------------------|
| 20 | 29.59 |
| 10 | 29.56 |
| 5 | 29.56 |

b) Altering parameter L , which is the distance between the contacts (Table V). The results demonstrate that parameter L has almost no effect on the maximal electric field strength in disconnectors.

TABLE V. THE RELATION BETWEEN PARAMETER L AND THE MAX ELECTRIC FIELD STRENGTH

| Parameter L (mm) | E_{max} (kV/mm) |
|--------------------|-------------------|
| 180 | 29.59 |
| 190 | 29.33 |
| 200 | 29.20 |

c) Structural parameters h , R_1 and R_2 of the shield are rather significant to the electric field distributions, so these three parameters are considered together. In Table VI the electric field distributions in disconnectors can be more uniform owing to the change of these three parameters.

TABLE VI. RELATION BETWEEN PARAMETERS h , R_1 AND R_2 AND THE MAXIMAL ELECTRIC FIELD STRENGTH E_{max}

| No. | h (mm) | R_1 (mm) | R_2 (mm) | E_{max} (kV/mm) |
|-----|----------|------------|------------|-------------------|
| 1 | 121 | 60 | 95 | 24.67 |
| 2 | 121 | 60 | 150 | 24.72 |
| 3 | 111 | 25 | 95 | 29.59 |

Based on the aforementioned analysis, it is concluded that parameters t and L have almost no effect on the field distributions, but parameters h , R_1 and R_2 are vital, namely, the structural parameters of the shield have more effect on the

field distributions. So, parameters h , R_1 and R_2 should be selected as design variables.

VI. OPTIMUM SHAPE DESIGN OF DISCONNECTORS

The shape design optimization mathematical equations of disconnector model can be described as follows.

$$\min f(x_1, x_2, x_3) = E_{\max} \quad (24)$$

where E_{\max} is the maximal electric field strength value, x_1 , x_2 and x_3 represents the parameters h , R_1 , and R_2 in Figure 2, respectively.

The regions of the design variables are listed as follows according to the relative working experience.

$$\begin{cases} 110 \leq h \leq 150 \\ 20 \leq R_1 \leq 60 \\ 60 \leq R_2 \leq 120 \end{cases} \quad (25)$$

The values of design variables and the code of central composite design are listed in Table VII and VIII respectively. The α value is 1.216.

TABLE VII. THE INITIAL VALUES OF DESIGN VARIABLES

| Design variable | Code | $-\alpha$ | -1 | 0 | +1 | $+\alpha$ |
|-----------------|-------|-----------|-----|-----|-----|-----------|
| h (mm) | x_1 | 117.8 | 120 | 130 | 140 | 142.2 |
| R_1 (mm) | x_2 | 27.8 | 30 | 40 | 50 | 52.2 |
| R_2 (mm) | x_3 | 77.8 | 80 | 90 | 100 | 102.2 |

TABLE VIII. THE CODES OF CENTRAL COMPOSITE DESIGN COMPRISING THREE DESIGN VARIABLES

| No. | Design points | | | Code points | | |
|-----|---------------|------------|------------|-------------|-----------|-----------|
| | h /mm | R_1 (mm) | R_2 (mm) | x_1 | x_2 | x_3 |
| 1 | 120 | 30 | 80 | -1 | -1 | -1 |
| 2 | 120 | 30 | 100 | -1 | -1 | +1 |
| 3 | 120 | 50 | 80 | -1 | +1 | -1 |
| 4 | 120 | 50 | 100 | -1 | +1 | +1 |
| 5 | 140 | 30 | 80 | +1 | -1 | -1 |
| 6 | 140 | 30 | 100 | +1 | -1 | +1 |
| 7 | 140 | 50 | 80 | +1 | +1 | -1 |
| 8 | 140 | 50 | 100 | +1 | +1 | +1 |
| 9 | 130 | 40 | 90 | 0 | 0 | 0 |
| 10 | 117.8 | 40 | 90 | $-\alpha$ | 0 | 0 |
| 11 | 142.2 | 40 | 90 | $+\alpha$ | 0 | 0 |
| 12 | 130 | 27.8 | 90 | 0 | $-\alpha$ | 0 |
| 13 | 130 | 52.2 | 90 | 0 | $+\alpha$ | 0 |
| 14 | 130 | 40 | 77.8 | 0 | 0 | $-\alpha$ |
| 15 | 130 | 40 | 102.2 | 0 | 0 | $+\alpha$ |

The results can be obtained by calculating the design values using the FEM in turn. Based on the second order model, the response surface model can be obtained as follows:

$$f(x_1, x_2, x_3) = 26.81 - 1.78x_1 - 0.62x_2 + 0.55x_3 - 0.05x_1x_2 + 0.13x_1x_3 - 0.13x_2x_3 + 0.21x_1^2 + 0.3x_2^2 - 0.25x_3^2 \quad (26)$$

Equation (26) can be solved using sequential quadratic programming, and the optimal results are shown in Table IX. The electric potential distributions and electric field distributions in the disconnector with optimum structural parameters have been depicted in Figure 4 using FEM.

TABLE IX. THE CONTRAST BETWEEN THE INITIAL AND OPTIMAL RESULTS

| Parameters | h /mm | R_1 /mm | R_2 /mm | E_{\max} (kV·mm ⁻¹) |
|---------------|---------|-----------|-----------|-----------------------------------|
| Optimal value | 138.16 | 33.96 | 86.76 | 22.90 |
| Initial value | 111 | 25 | 95 | 29.59 |

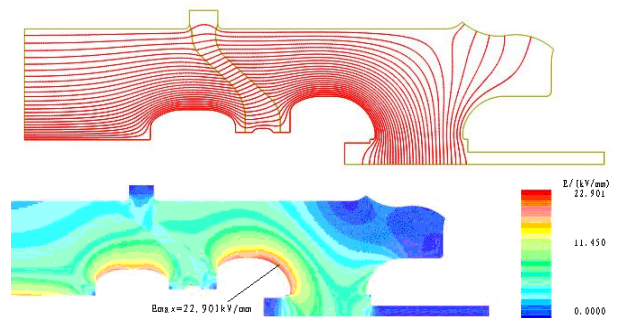


Fig. 4. The potential and electric field distributions in the disconnector with optimum structural parameters

As shown in Figure 4 and Table IX the maximum electric field strength is 22.9kV/mm, lower than the allowable electric field strength 24.0kV/mm. So the optimal results meet the design requirements, increase the withstanding voltage, and improve the reliability of disconnectors.

VII. CONCLUSION

In this paper, RSM coupled with FEM are successfully applied, for the first time, for the optimization of 550kV disconnector in GIS. The electric field distributions in 550kV disconnectors have been analyzed and calculated based on FEM in transient quasistatic electric field, through a FORTRAN code. Then the optimum shape design in 550kV disconnectors was completed based on the RSM coupled with FEM. The optimal results indicate that the electric field distributions in the optimized disconnector model are more uniform than those of the initial model. So, setting the optimal structural parameters in electric devices is feasible and highly efficient using RSM coupled with FEM. The proposed disconnector model with optimum structure parameters has undertaken all withstanding voltage tests. The work discussed in this paper can be employed to improve the insulation performance and operational reliability of 550kV disconnectors in gas insulated switchgears.

REFERENCES

[1] G. Zhang, Finite Element Method, Beijing, Mechanical Industry Press, 1991

- [2] J. Sheng, Numerical analysis of electromagnetic field. Xi'an, Xi'an Jiaotong University Press, 1991
- [3] Y. J. Kim, J. D. Lee, B. J. Lee, H. K. Shin, S. C. Hahn, "Design optimization of permanent magnetic actuator for vacuum circuit breaker by response surface method", International Conference on Electrical Machines and Systems (ICEMS), pp. 1-4, Saporu, Japan, October 21-24, 2012
- [4] K. W. Jeon, T. K. Chung, S. C. Hahn, "NEMA class a slot shape optimization of induction motor for electric vehicle using response surface method", International Conference on Electrical Machines and Systems (ICEMS), pp. 1-4, Beijing, China, August 20-23, 2011
- [5] B. H. Lee, K. S. Kim, J. P. Hong, J. H. Lee, "Optimum shape design of single-sided linear induction motors using response surface methodology and finite-element method", International Conference on Electrical Machines and Systems (ICEMS), pp. 1-5, Beijing, China, August 20-23, 2011
- [6] L. Egiziano, V. Tucci, C. Petrarca, M. Vitelli, "A Galerkin model to study the field distribution in electrical components employing nonlinear stress grading materials", IEEE Transactions on Dielectrics and Electrical Insulation, Vol. 6, No. 6, pp. 765-773, 1999
- [7] J. Kuang, J. D. Lavers, S. Boggs, "Program for transient nonlinear finite element analysis with applications to coupled field programs", 10th International Symposium on High Voltage Engineering, Montreal Quebec, Canada, pp. 25-29, 1997
- [8] X. Ma, Electromagnetic theory and applications, Xi'an, Xi'an Jiaotong University Press, 2000
- [9] G. Lupo, G. Miano, V. Tucci, M. Vitelli. "Field distribution in cable terminations from a quasi-static approximation of the Maxwell equations", IEEE Transactions on Dielectrics and Electrical Insulation, Vol. 3, No. 3, pp. 399-409, 1996
- [10] Z. Zhang, B. Xiaofeng, "Comparison about the three central composite designs with simulation. advanced computer control", International Conference on Advanced Copmputer Control (ICACC), Singapore, pp. 163-167, January 22-24, 2009
- [11] C. Petrarca, L. Egiziano, V. Tucci, M. Vitelli "Impulse performances of cable terminations employing stress grading accessories", 1999 Annual Report Conference on Electrical Insulation and Dielectric Phenomena, Austin, USA, Vol. 1, pp. 146-149, October 17-20, 1999
- [12] B. Li, SF6 High Voltage Apparatus, Beijing, Mechanical Industry Press, 2008